Investigation of photoluminescence in the InGaAs/GaAs system with 1100-nm range quantum dots

© A.V. Babichev[1], S.D. Komarov[2], Yu.S. Tkach[1], V.N. Nevedomskiy[1], S.A. Blokhin[1], N.V. Kryzhanovskaya[2,3], A.G. Gladyshev[4], L.Ya. Karachinsky[4], I.I. Novikov[4]

[1] Ioffe Institute,
194021 St. Petersburg, Russia
[2] Alferov Federal State Budgetary Institution of Higher Education and Science
Saint Petersburg National Research Academic University of the Russian Academy of Sciences,
194021 St. Petersburg, Russia
[3] ITMO University,
190008 St. Petersburg, Russia
[4] National Research University Higher School of Economics,
197101 St. Petersburg, Russia

E-mail: a.babichev@mail.ioffe.ru

Received October 7, 2022
Revised January 31, 2023
Accepted February 3, 2023

The results of studying the optical properties of InGaAs quantum dots are presented. Single-layer InGaAs quantum dots with a height of 5.3, 3.6 and 2.6 monolayers, as well as three-stacked layers of tunnel-uncoupled quantum dots with a height of 2.6 monolayers were formed by molecular-beam epitaxy according to the Stransky–Krastanov mechanism on GaAs substrates, using the partial capping and annealing technique. A decrease in the size of quantum dots makes it possible to carry out a blueshift of the photoluminescence spectrum maximum from 1200 nm to 1090 nm, and an increase in the number of QD layers makes it possible to compensate for the decrease in the peak intensity. It is shown that this type of quantum dots is suitable for creating the lasers active regions with a vertical microcavity for neuromorphic computing.

Keywords: molecular-beam epitaxy, gallium arsenide, InGaAs, Stranski–Krastanow mode.

DOI: 10.21883/SC.2023.01.55622.4184

1. Introduction

Quantum dots (QDs) are used as active regions for a wide range of laser applications [1], including in lasers with a microresonator for neuromorphic computing [2,3]. In single photon sources, a low QD density is required [4], however, in laser structures with a vertical microresonator, where initially the volume of the active region is minimal, on the contrary, it is necessary to increase the QD density in order to reach the laser generation threshold. The optical gain of the active regions based on „ideal" QD should exceed the optical gain of the active regions based on quantum wells, but in practice the situation is different, due to the effect of inhomogeneous broadening in the ensemble of QDs. This fact limits the high-temperature generation of QD lasers in a structure with a vertical microresonator. The maximum operating temperature of these current-pumped lasers is ~ 100 K [5].

InAs/InGaAs CT [6] are traditionally used for epitaxial growth of long-wave laser structures with QD (O-spectral range, near 1300 nm). In turn, the deposition of an additional InGaAs layer with a lower indium composition makes it possible to realize long-wave radiation in QD based on triple solid solutions of InGaAs [7]. However, the amplifying properties of the active regions of the O-spectral range based on InGaAs QD are lower in comparison with the case of using InAs QD. QDs are epitaxially grown in the Stransky–Krastanov (SK) mode, for which the presence of a wetting layer [8] is typical, which is essentially a strained QA with a height of several nanometers located on the heterointerface CT/GaAs [9].

InGaAs/GaAs QD are traditionally used to implement laser structures with radiation near 1100 nm. With a high proportion of indium ($\sim 60\%$), mechanically highly stressed „lenticular" InGaAs QD with dimensions of $10-15$ nm and a point density of $\sim (1-2) \cdot 10^{11}$ cm^{-2} are formed. Reduction of the proportion of indium to 45% reduces the QD density to $(1-2) \cdot 10^{9}$ cm^{-2} and increases the QD size to $20-25$ nm [10]. A further decrease of the proportion of indium (up to 30%) allows for a significant reduction of the mechanical stresses between the deposited layer and the substrate (up to 2%), to deposit QD with a lower density ($\sim 9 \cdot 10^{9}$ cm^{-2}) and elongated along one crystallographic direction, which is required to create sources of single photons. In this case, the characteristic QD dimensions are in the range of $50-100$ nm along the direction $[0\bar{1}1]$ and ~ 30 nm in the perpendicular direction [11–15].

The typical half-width of the photoluminescence spectrum (PL) of QD emitting near 1100 nm and demonstrating the high efficiency of FL required for laser applications is $80-90$ MeV [16,17], which significantly exceeds the similar value for QD O-spectral range [18]. This fact is due to a greater fluctuation in the size of QD in the ensemble for the case of QD of the spectral range 1100 nm, whose sizes

are smaller in comparison with QD of the spectral range 1200−1300 nm at typical growth temperatures. In turn, the implementation of low-temperature QD allows to reduce the half-width of the PL line (up to 35−40, MeV [16,17]), however, the intensity of the PL line drops by several orders of magnitude [16].

To implement photonic reservoir calculations, it is required to form a dense array of spectrally homogeneous microlasers in order to implement diffraction binding of lasers in the [2] array. An increase in the number of microlazers in the array results in the increase of the threshold power of optical pumping required for the implementation of photonic reservoir calculations. As a result, along with the spectral uniformity of microlasers, it is also necessary to minimize the threshold pumping power of individual microlasers [2]. On the one hand, it is necessary to increase the gain of active areas based on QD for reducing the threshold power, and on the other hand, it is necessary to minimize losses in the layers of distributed Bragg reflectors.

Approaches aimed at reducing inhomogeneous linewidth broadening, i. e. QDs size distribution are applied to increase the maximum optical gain of active regions in lasers of the spectral range of 1100 nm based on QD [17].

The first of the approaches to reduce inhomogeneous linewidth broadening is to use submonolayer migration-stimulated epitaxy (submonolayer deposition) based on the formation of alternating submonolayer layers InAs/(In)GaAs [11–13,19,20]. It is worth noting the complexity of controlling the composition of QD among the disadvantages of the approach due to the inertia of switching the dampers of materials in molecular beam epitaxy (MBE) units.

The second approach to reduce QD inhomogeneous linewidth broadening is to use the partial capping and annealing technique (PCA) or indium-flush procedure as this method is also called [21], QD height-limiting growth method [17]. In this case, the structure is annealed for several minutes after the formation of QD and epitaxy of a thin coating layer of GaAs [22–24]. During annealing of the structure, the height of the QD is reduced due to desorption of the material from the uncovered area near the top of the QD. The development of this approach is presented in the paper [25], in which, due to the formation of an additional wide-band layer of AlAs after the formation of QD, it was possible to eliminate the binding effect between QD and the wetting layer states (the presence of PL from the wetting layer in the PL spectra of the QD ensemble), and high-temperature annealing was applied to reduce the spread in the height of QD in the ensemble.

To summarize: the use of the PCA method for QD epitaxy in lasers with a vertical microresonator allows for more precise control of the radiation wavelength (by changing the thickness of the coating layer and by changing the annealing time) and, as a result, more precise control of the amount of detuning between the spectral position of the radiation of the QD ensemble and the spectral position of the main optical mode of the resonator what is required for laser structures used for neuromorphic computing.

Previously, the method of organometallic vapor phase epitaxy (OMVPE) was used to form heterostructures of QD lasers with a vertical microresonator required for neuromorphic calculations [2,3]. However, the typical deviation of layer thicknesses over the area of the epitaxial structure was $\sim 2\%$, which led to a shift in the resonant wavelength of the radiation ~ 30 MeV over the area of the two-inch plate. As a result, when creating lasers for photonic reservoir calculations, it is necessary to compensate for this spectral inhomogeneity. In turn, the MBE technology provides greater uniformity of the composition and thickness of the layers over the area of the structure ($\sim 1\%$).

This paper presents the results of epitaxial growth and the study of the optical properties of InGaAs QD grown by the MBE method using the Stransky–Krastanov mechanism using the PCA method.

2. Experimental samples

During the experiment, a series of samples including InGaAs QD grown by the Stransky–Krastanov mechanism was formed by the MBE method. A buffer anti-aging layer of GaAs with a thickness of 100 nm was grown on GaAs(100) substrates. There was a layer of the GaAs matrix with a thickness of 300 nm between the two barrier layers $Al_{0.23}Ga_{0.77}As$ with a thickness of 35 nm in the middle of which layers with QD were placed. The growth temperature was 580°C for all studied structures. In turn, before the deposition of QD, the substrate temperature decreased to 490°C. The deposition rate of QD layers was 0.2 monolayer (ML) per second. Next, the deposition of the capping layer of GaAs with an increase in the arsenic flow and the subsequent temperature rise to 580°C [17] was performed for annealing the samples for 4 min (implementation of the PCA mode).

Structures 1−3 included one layer $In_{0.65}Ga_{0.35}As$ QD with different QD heights (5.3, 3.6 and 2.6 ML). The thickness of the GaAs layer covering QD in them was 5.0 nm. The structure of 4 is similar to the structure of 3, except for the thickness of the GaAs layer covering the QD, which has been reduced to 3.5 nm.

A structure 5 with three layers of $In_{0.63}Ga_{0.37}As$ QD with a height of 2.6 ML was grown for increasing the optical amplification of the active regions of lasers with a vertical microresonator required for neuromorphic calculations. A further increase in the number of QD layers to 5 or more is inefficient due to the need to place the QD in the maximum spatial distribution of the intensity of the standing wave in the microresonator. The thickness of the GaAs layer covering the QD in the structure 5 was 5 nm, and the QD layers were separated by GaAs layers with a thickness of 20 nm in order to exclude the binding effect between the QD layers. An exposure was added for structures 3−5, after QD deposition on the GaAs surface, the exposure time in the arsenic stream was 30 s.

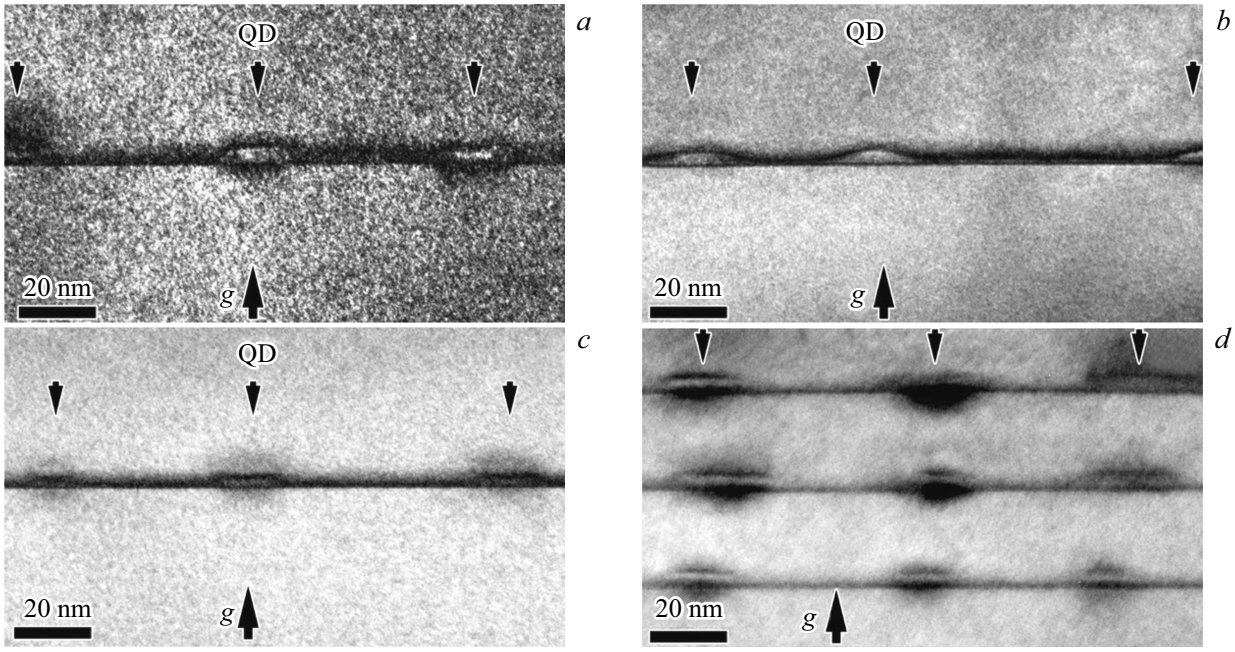

Figure 1. Cross-sectional images $(1\bar{1}0)$: *a, b, c* and *d* — for structures 1, 2, 3 and 5, respectively.

Transmission electron microscopy (TEM) studies were performed using JEM2100F (Jeol) electron microscope with an accelerating voltage of 200 kV. The samples were prepared in cross-sectional geometry using a generally accepted technique, including thinning by precision grinding and spraying with argon ions at the final stage before perforation.

Measurements of the PL spectra at a temperature of 297 K were performed using the PM2000, VerteX (Nanometrics) unit using an InGaAs photodetector and a semiconductor laser with a pump wavelength of 532 nm. The measurement speed was 5 points per second, the gap size 2 mm. A diffraction grid of 300 lines/mm was used. The optical pumping power is fixed at the level of 4 and 45 MW, respectively.

The PL micro-spectra were measured in the temperature range of 77–290 K using an Nd:YLF laser with a wavelength of 527 nm. The laser power varied in the range of 0.016–2 MW (continuous pumping mode). The radiation was focused using a 100× M lens,Plan Apo NIR (Mitutoyo). The spot size after focusing was ~ 1 microns. The PL signal was directed to the input slots of the MS5204i monochromator (Sol Instruments). The technique of synchronous detection using a cooled InGaAs detector was used to register the spectra of micro-PL.

3. Results and discussion

Figure 1 shows images of structures 1–3, 5, obtained by transmission electron microscopy (TEM images) under two-beam conditions with an active diffraction vector $g = (002)$ in the dark field mode. It is shown that QD in the structure of 3 have the lowest height. The shape of the QD differs from sample to sample. In structure 2 QDs have the shape of lenses with a height of ~ 4 nm and a lateral size of 20–27 nm. In structure 1, the QD shape is a „high" truncated pyramid, and in structure 3 is also a truncated pyramid, but with a significantly smaller height. This form of QD is determined by the use of annealing after the growth of the covering layer of GaAs, which led to the evaporation of indium from the apexes of the QD protruding above the covering layer. InGaAs layer parameters are listed in the table. The estimated value of QD density in the studied samples was $(1-3) \cdot 10^{10}$ units/cm^2. The upper boundary of the GaAs layers that covered the QD during annealing between QD is not visible. However, the layers in which QDs are located have a rather strong dark contrast. A similar contrast is associated with the wetting layer (WL), which remains after the formation of QD. The thickness of this „dark" layer on TEM images reaches 3.5–4.0 nm in the studied structures. Typical thicknesses of the wetting layer with InAs QD growth are 0.5–1.0 nm [26]. Thus, with the growth of InGaAs QD, the thickness of the wetting layer exceeds the same value in InAs QD [12], which is due to a smaller mismatching in the crystal lattice constant between InGaAs and the GaAs matrix layer [27], in fact, the composition of indium InGaAs.

Fig. 1, *d* shows the results of a study of the structure 5, including 3 layers $In_{0.63}Ga_{0.37}As$ QD height 2.6 ML. The figure shows a vertical alignment of QD during storage. As shown earlier [28], successive deposition of several layers of QD separated by thin barriers results in the fact that the mechanical stresses of the lower layer of QD affect the growth of the next layer of QD and the effect of vertical

InGaAs QD parameters of grown structures

№ structures	Height QD, nm	Lateral QD size, nm	Thickness wetting layer, nm
1	4.5–5.5	15–20	4.9
2	2.0–4.0	20–27	2.8
3	2.0–2.5	14–23	1.5–2.4
5	3.8–4.2	18–35	1.5–1.7

alignment of QD in columns is observed. At the same time, it is shown [29] that this effect is observed at the thicknesses of layers separating CT, < 15 nm. In turn, in the structure 5, the thickness of the layers separating the QD is higher (20 nm), but at the same time the effect of storage in columns is also observed, which may be due to the larger lateral size of the QD. Based on the statistical analysis of a number of images obtained for the structure 5, it was shown that the shape and size of the QD in all three layers are identical, while the growth mode of the QD layers was also the same. No special approaches were used to preserve the QD size. Thus, with these QD sizes and thicknesses of the separating GaAs layers, during growth, the elastic stress field from the already grown QD has an effect only on the location of the QD in the formed layer and does not affect their size and shape in any way. As a result, the effect of an increase of the magnitude of inhomogeneous linewidth broadening due to the size dispersion of QD in different rows does not manifest itself.

Fig. 2 shows the PL spectra measured at the optical pumping level of 4 and 45 MW. At a low pump level, the structure 1 with a single layer $In_{0.65}Ga_{0.35}As$ with a QD height of 5.3 ML demonstrates the maximum intensity of the PL spectrum near 1198 nm with a small full half-width of the maximum of the PL spectrum ($\sim$ 45 MeV, Fig. 1, *a*). Thus, the use of the root cause analysis (RCA) technique allowed to reduce the spread of QD parameters (heterogeneous broadening in the QD ensemble [20,30]). The value of the PL full width at half maximum (FWHM value) corresponding to the transitions through the ground states in the QD ensemble ($\sim$ 38 MeV, based on the decomposition into 2 Gaussian components) is comparable with the previously obtained results (FWHM $\sim$ 40 MeV) for $In_{0.5}Ga_{0.5}As$ QD of similar height obtained by RCA [17]. A short-wave shoulder near 1154 nm is also observed in the PL spectrum, 42 MeV away from the PL line corresponding to transitions through ground states. Typical energy distances between the ground and excited states in the QD ensemble are 25–75 MeV and are determined by epitaxy modes, including the deposition temperature of QD, their composition, as well as the thickness of the covering layer [21].

A decrease in the QD height from 5.3 to 2.6 ML (structures 1–3) leads to a short-wave shift in the position of the maximum intensity of the PL spectrum, an increase in the intensity of the PL line corresponding to transitions through excited states, as well as to a broadening of the maximum of the spectrum PL.

The maximum intensity of the PL spectrum for the structure is 3 with a QD height of 2.6 ML corresponds to the radiation wavelength of 1094 nm. As shown earlier [31], a decrease in the size of QD while maintaining their composition leads to an increase in the quantization energy of the ground and excited states. When a certain critical size of the QD is reached, the excited states rise in energy so much that they shift to the region of the wetting layer, leading to the presence of only the ground state and optical transitions associated with it. In turn, an increase in the size of the QD above some critical value leads to a convergence of energy levels until a mini-zone is formed. Thus, with a decrease in the size of the QD, two effects manifest themselves: a short-wave shift in the position of both PL lines, as well as an increase in the energy distance between these PL lines [1] (a larger short-wave shift of the excited state PL line relative to the shift of the ground state PL line), which is described by the short-wave shift of the position of the maximum PL, as well as an increase in the width of the maximum spectrum PL.

The structure 5 with three layers $In_{0.63}Ga_{0.37}As$ a 2.6 MS QD shows a higher intensity of the PL spectrum compared to the structure 3 with a single layer of 2.6 ML QD. It was previously shown [32] that the effect of saturation of PL through ground states is observed at higher optical pumping densities in structures with several layers of QD, which correlates with the experiment. The full width of the PL spectrum from QD is slightly lower than the same value for a structure of 3 with one QD layer due to more efficient pumping of the ground state in a structure of 5 with three layers of QD.

Earlier it was reported about the use of a coating layer with a thickness of 3 nm for the implementation of QD emitting in the spectral range of 1100 nm, grown by the MPE [17] method. Similar parameters were used for the growth of the structure 4, where the thickness of the coating layer was up to 3.5 nm. However, a decrease in the thickness of the coating layer in comparison with structures 1–3 led to the absence of a line typical for QD in the PL spectrum (see Fig. 1, *a*). In the PL spectrum of structure 4, there are three lines corresponding to GaAs (near 860 nm), the InGaAs wetting layer (near 910 nm, designation WL), as well as the QD layer significantly shifted to the short-wavelength region relative to the position of the QD line in the structure 3. Due to the reduction of the thickness of the covering layer, large QD has reevaporated and radiation from QD with smaller dimensions radiating in the shorter wavelength region of the spectrum is observed in the PL spectrum. The intensity of PL from QD decreased, which is associated with a lower density of QD compared to the structure 3.

An increase in the level of optical pumping (up to 45 MW) leads to an increase in the intensity of PL. In contrast to the case of low optical pumping, two maxima are clearly expressed in the FL spectrum of the structure 1

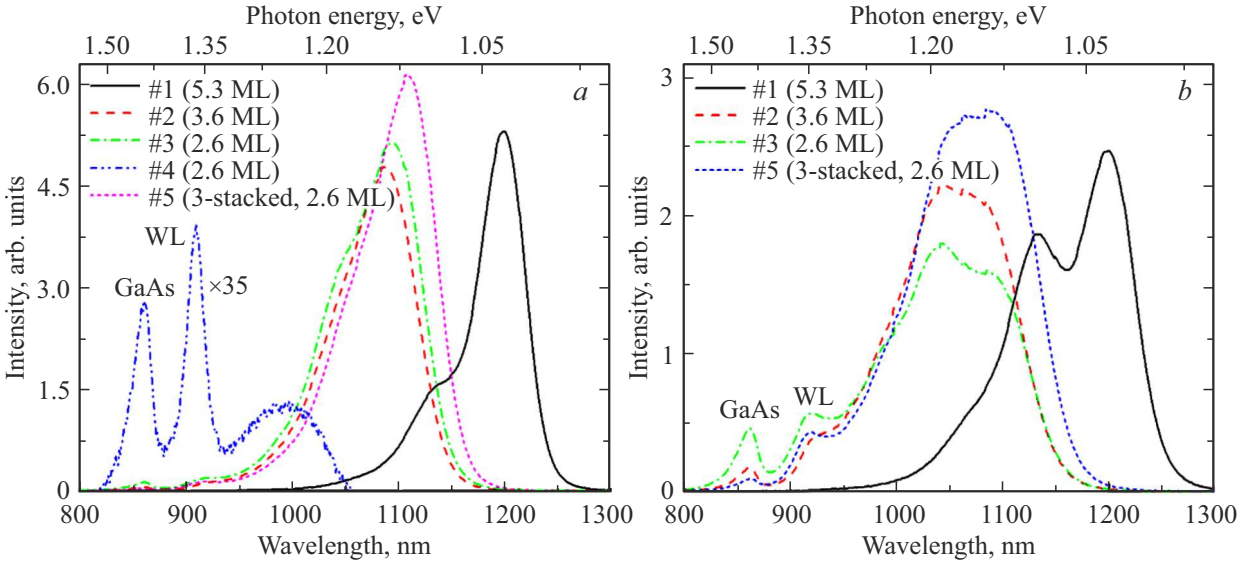

Figure 2. Photoluminescence spectra of structures 1–5 at the optical pumping level of 4 MW (panel *a*) and 45 MW (panel *b*). The spectrum of the PL structure 4 on panel a is shown in scale (×35), the designation WL corresponds to the InGaAs wetting layer.

with a single layer $In_{0.65}Ga_{0.35}As$ CT, which is due to more efficient pumping of excited states (Fig. 1, *b*). With a decrease in the QD height (from 5.3 to 2.6 ML), two effects are observed: a decrease in the intensity of the maximum of the PL spectrum, as well as an increase in the intensity of the line corresponding to transitions through excited states. The structure 5 with three layers of QD demonstrates an increase in the intensity of the PL spectrum and more efficient pumping of the ground state in comparison with the structure 3 with one layer of QD. Comparison of the PL spectra of the structure 1 with one QD layer with a height of 5.3 ML and the structure 5 with three QD layers with a height of 2.6 ML allows drawing the following conclusions: reducing the size of the QD allows a short-wave shift of the position of the maximum of the PL spectrum from 1200 to 1090 nm, and increasing the number of QD layers allows for compensation for the drop in intensity of the maximum of the PL spectrum.

Temperature studies of the spectra of micro-PL structure 5 with three layers of QD 2.6 ML high were performed. Fig. 3 shows the results of measurements at an optical pumping power of 0.17 MW. At a temperature of 77 K, a broad maximum is observed with a characteristic full width at half maximum micro-PL spectrum ~ 110 MeV. An increase in temperature to 140 K leads to an increase in the intensity of micro-PL. At the same time, a drop in the value of the full width at half maximum of the micro-PL spectrum, which is due to more efficient pumping through the ground states. A further increase of the temperature to 290 K results in the decrease of the radiation intensity. A small drop of the integral intensity of micro-PL (by 1.9 times) with an increase of temperature from 77 to 290 K indicates a high optical quality of the formed QDs. The maximum of the spectrum of micro-PL, corresponding to a temperature

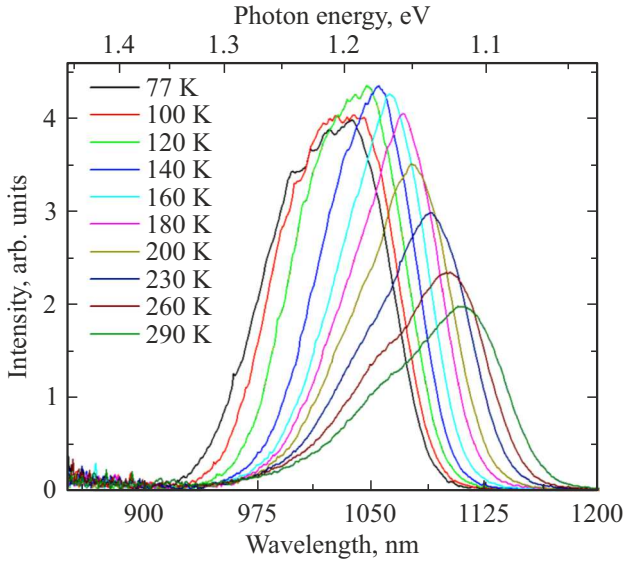

Figure 3. Spectra of micro-PL structure 5, measured at various temperatures. The optical pumping power was 0.17 MW.

of 290 K, is decomposed into two Gaussian components. The FWHM of the PL line near 1070 nm corresponding to transitions through the ground states was ~ 54 MeV. The energy distance between the ground and excited states in the QD ensemble was 47 MeV.

Figure 4 shows the spectra of the micro-PL structure 5 with 3 QD layers with height of 2.6 ML, depe nding on the pumping, measured at a temperature of 290 K. With a pumping power of 0.02 MW, optical pumping is observed through the ground states in the QD ensemble. The PL peak FWHM was 66 MeV. An increase of the intensity of the micro-PL line from excited states is observed with an

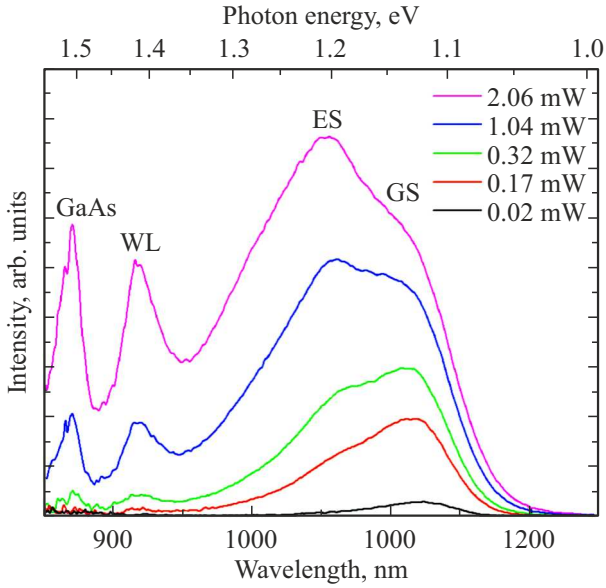

Figure 4. Spectra of micro-PL structure 5 at different levels of optical pumping, measured at a temperature of 290 K.

increase in pumping, the luminescence efficiency from the wetting layer and the substrate increases. With a pumping level of 0.54 MW, the intensities of micro-PL lines from transitions in the QD ensemble through the ground and excited states are compared. A further increase of the pumping level (> 0.54 MW) leads to a faster increase of the intensity of the PL line due to optical transitions through excited states with saturation of the intensity of the PL line due to optical transitions through ground states.

4. Conclusion

Epitaxial growth experiments and investigation of the optical properties of InGaAs QD in the spectral range of 1100 nm produced by the Stransky–Krastanov mechanism using the method of partial covering and high-temperature annealing of QD were performed. The structural quality of the formed QD was studied by the transmission electron microscopy. It was shown that a vertical alignment of QD is observed during storage for a structure comprising three layers $In_{0.63}Ga_{0.37}As$ QD with a height of 2.6 ML. The PL spectra of the formed structures were studied. A reduction of the size of the QD allows for short-wave shift of the position of the maximum of the PL spectrum from 1200 to 1090 nm, and an increase of the number of QD layers allows compensating for the decrease of the intensity of the maximum of the PL spectrum. Temperature studies of the spectra of micro-PL structures with three layers of QD with a height of 2.6 ML were conducted. A slight drop of the integral intensity of micro-PL was found in case of an increase of temperature from 77 to 290 K, which indicates the high optical quality of the formed QD and the prospects of using QD data as active regions of lasers with a vertical microresonator for neuromorphic calculations.

Funding

The study of the authors from the A.F. Ioffe Institute of Physics and Technology of the Russian Academy of Sciences was financed by a grant from the Russian Science Foundation No. 22-19-00221, https://rscf.ru/project/22-19-00221/ in terms of design development, epitaxy of heterostructures, TEM studies, study of microphotoluminescence spectra. N.V. Kryzhanovskaya is grateful for the support of the Fundamental Research Program of the National Research University „Higher School of Economics“ regarding the analysis of photoluminescence spectra.

Conflict of interest

The authors declare that they have no conflict of interest.

References

[1] D. Bimberg, M. Grundmann, N. N. Ledentsov. *Quantum Dot Heterostructures* (Chichester, England, John Wiley & Sons Ltd, 1999) p. 344.
[2] T. Heuser, J. Grose, S. Holzinger, M.M. Sommer, S. Reitzenstein. IEEE J. Select. Top. Quant. Electron., **26** (1), 1 (2020).
[3] T. Heuser, J. Große, A. Kaganskiy, D. Brunner, S. Reitzenstein. APL Photonics, **3** (11), 116103 (2018).
[4] I.I. Novikov, A.M. Nadtochiy, A.Yu. Potapov, A.G. Gladyshev, E.S. Kolodeznyi, S.S. Rochas, A.V. Babichev, V.V. Andryushkin, D.V. Denisov, L.Ya. Karachinsky, A.Yu. Egorov. J. Luminesc., **239**, 118393 (2021).
[5] S. Reitzenstein, T. Heindel, C. Kistner, A. Rahimi-Iman, C. Schneider, S. Höfling, A. Forchel. Appl. Phys. Lett., **93** (6), 061104 (2008).
[6] A. Rantamäki, G.S. Sokolovskii, S.A. Blokhin, V.V. Dudelev, K.K. Soboleva, M.A. Bobrov, A.G. Kuzmenkov, A.P. Vasil'ev, A.G. Gladyshev, N.A. Maleev, V.M. Ustinov, O. Okhotnikov. Optics Lett., **40** (14), 3400 (2015).
[7] J. Große, P. Mrowiński, N. Srocka, S. Reitzenstein. Appl. Phys. Lett., **119** (6), 061103 (2021).
[8] X. Hu, Y. Zhang, D. Guzun, M.E. Ware, Y.I. Mazur, C. Lienau, G.J. Salamo. Sci. Rep., **10** (1), 10930 (2020).
[9] G. Sęk, P. Poloczek, K. Ryczko, J. Misiewicz, A. Löffler, J.P. Reithmaier, A. Forchel. J. Appl. Phys., **100** (10), 103529 (2006).
[10] A. Löffler. „*Selbstorganisiertes Wachstum von (Ga)InAs/GaAs-Quantenpunkten und Entwicklung von Mikroresonatoren höchster Güte für Experimente zur starken Exziton-Photon-Kopplung*“, Dissertation (Würzburg, Germany, 2008) p. 191. https://opus.bibliothek.uni-wuerzburg.de/frontdoor/index/index/year/2008/docId/2589 URN: urn:nbn:de:bvb:20-opus-30323.
[11] A. Löffler, J.P. Reithmaier, G. Sęk, C. Hofmann, S. Reitzenstein, M. Kamp, A. Forchel. Appl. Phys. Lett., **86** (11), 111105 (2005).
[12] P. Poloczek, G. Sęk, J. Misiewicz, A. Löffler, J.P. Reithmaier, A. Forchel. J. Appl. Phys., **100** (1), 013503 (2006).

[13] S. Reitzenstein, S. Münch, P. Franeck, A. Rahimi-Iman, A. Löffler, S. Höfling, L. Worschech, A. Forchel. Phys. Rev. Lett., **103** (12), 127401 (2009).
[14] C. Hopfmann, A. Musiał, M. Strauß, A. M. Barth, M. Glässl, A. Vagov, M. Strauß, C. Schneider, S. Höfling, M. Kamp, V.M. Axt, S. Reitzenstein. Phys. Rev. B, **92** (24), 245403 (2015).
[15] A. Löffler, J.-P. Reithmaier, A. Forchel, A. Sauerwald, D. Peskes, T. Kümmell, G. Bacher. J. Cryst. Growth, **286** (1), 6 (2006).
[16] N. Ozaki, S. Kanehira, Y. Hayashi, S. Ohkouchi, N. Ikeda, Y. Sugimoto, R.A. Hogg. J. Cryst. Growth, **477** (1), 230 (2017).
[17] K. Watanabe, T. Akiyama, Y. Yokoyama, K. Takemasa, K. Nishi, Y. Tanaka, M. Sugawara, Y. Arakawa. J. Cryst. Growth, **378**, 627 (2013).
[18] R.P. Mirin, K.L. Silverman, D.H. Christensen, A. Roshko. J. Vac. Sci. Technol., B: Microelectron. Nanometer Struct., **18** (3), 1510 (2000).
[19] T. Finke, V. Sichkovskyi, J.P. Reithmaier. J. Cryst. Growth, **517**, 1 (2019).
[20] S. Ruvimov, P. Werner, K. Scheerschmidt, U. Gösele, J. Heydenreich, U. Richter, N.N. Ledentsov, M. Grundmann, D. Bimberg, V.M. Ustinov, A.Yu. Egorov, P.S. Kop'ev, Zh.I. Alferov. Phys. Rev. B, **51** (20), 14766 (1995).
[21] H. Sasakura, S. Kayamori, S. Adachi, S. Muto. J. Appl. Phys., **102** (1), 013515 (2007).
[22] L. Wang, A. Rastelli, O. G. Schmidt. J. Appl. Phys., **100** (6), 064313 (2006).
[23] Z.R. Wasilewski, S. Fafard, J.P. McCaffrey. J. Cryst. Growth, **201–202**, 1131 (1999).
[24] J.M. García, T. Mankad, P.O. Holtz, P.J. Wellman, P.M. Petroff. Appl. Phys. Lett., **72** (24), 3172 (1998).
[25] M.C. Löbl, S. Scholz, I. Söllner, J. Ritzmann, T. Denneulin, A. Kovács, B.E. Kardynał, A.D. Wieck, A. Ludwig, R.J. Warburton. Commun. Phys., **2** (1), 93 (2019).
[26] J.H. Blokland, M. Bozkurt, J.M. Ulloa, D. Reuter, A.D. Wieck, P.M. Koenraad, P.C.M. Christianen, J.C. Maan. Appl. Phys. Lett., **94** (2), 023107 (2009).
[27] P. Podemski, M. Pieczarka, A. Maryñski, J. Misiewicz, A. Löffler, S. Höfling, J.P. Reithmaier, S. Reitzenstein, G. Sęk. Superlat. Microstruct., 93, 214 (2016).
[28] N.N. Ledentsov, V.A. Shchukin, M. Grundmann, N. Kirstaedter, J. Böhrer, O. Schmidt, D. Bimberg, V.M. Ustinov, A.Yu. Egorov, A.E. Zhukov, P.S. Kop'ev, S.V. Zaitsev, N.Yu. Gordeev, Zh.I. Alferov, A.I. Borovkov, A.O. Kosogo, S.S. Ruvimov, P. Werner, U. Gösele, J. Heydenreich. Phys. Rev. B, **54**, 8743 (1996).
[29] S.A. Blokhin, A.M. Nadtochiy, A.A. Krasivichev, L.Ya. Karachinsky, A.P. Vasiliev, V.N. Nevedsky, M.V. Maksimov, G.E. Tsyrlin, A.D. Buravlev, N.A. Maleev, A.E. Zhukov, N.N. Lollipops, V.M. Ustinov. FTP, **47** (1), 87 (2013) (in Russian).
[30] V.I. Belyavsky, S.V. Shevtsov. FTP, **36** (7), 874 (2002). (in Russian).
[31] A. Schliwa, M. Winkelnkemper, D. Bimberg. Phys. Rev. B, **76** (20), 205324 (2007).
[32] M. Grundmann, D. Bimberg. Jpn. J. Appl. Phys., **36** (pt 1, No. 6B), 4181 (1997).

Translated by A.Akhtyamov